DOI: 10.1021/ma900104z

Macromolecules
ARTICLE

Highly Transparent and Refractive Polyimides with Controlled Molecular Structure by Chlorine Side Groups

Myeon-Cheon Choi,[†] Junji Wakita,[‡] Chang-Sik Ha,*[,†] and Shinji Ando*[,‡]

[†]*Department of Polymer Science and Engineering, Pusan National University, Busan 609-735, Korea, and* [‡]*Department of Chemistry and Materials Science, Tokyo Institute of Technology, Ookayama 2-12-1-S1-21, Meguro-Ku, Tokyo 152-8552, Japan*

Received January 17, 2009; Revised Manuscript Received May 25, 2009

ABSTRACT: Transparent polyimides (PIs) that have a high refractive index and low birefringence as well as good thermal and mechanical stability were synthesized by the judicious introduction of di- and tetrachlorinated aromatic diamines with aromatic/aliphatic dianhydrides. All the PI films, except for the PI derived from aromatic dianhydride and dichlorinated diamine (BPDA/2DCDB and BPDA/3DCDB), exhibited high optical transparency over the entire visible region. In particular, tetrachlorinated, fully aromatic polyimide (BPDA/TCDB) with a highly distorted conformation of the main chain exhibited excellent optical transparency in the visible range that was comparable to highly fluorinated aromatic PIs. This was attributed to the effective suppression of intra- and intermolecular charge transfer (CT) interactions by steric hindrance between the five-membered imide rings and chlorine atoms attached directly to the adjacent benzene rings as well as between chlorine atoms in the diamine molecules. A high transmittance of 82% at 400 nm with an average transmittance > 90% in the visible region and strong fluorescent emission were achieved in a fully aromatic PI (BPDA/TCDB). In addition, the chlorinated aromatic PIs exhibited high average refractive indices (1.702−1.732), suitable for applications as optical materials, such as microlens, and low birefringences (0.028−0.091) at 633 nm, due to the high atomic polarizability of chlorine and the bulky molecular structure of chlorinated PIs. In particular, a mean refractive index of 1.7018 was observed for BPDA/TCDB PI, which is extraordinarily high for a colorless PI.

Introduction

Colorless polymers with high thermal and mechanical stability as well as good optical transparency have been widely studied for applications in prospective flexible substrates of electronic devices and micro-optical devices in the field of displays, memory, lighting, solar cells, sensors, waveguides, etc., where glass is widely used.[1−3] To replace glass, polymers need to have the properties of glass, i.e., clarity, dimensional stability, thermal stability, barrier, solvent resistance, low coefficient of thermal expansion (CTE), and a smooth surface, as well as their inherently advantageous properties including light weight, flexibility, processability, and toughness. For example, polyesters such as poly(ethylene terephthalate) (PET) and poly(ethylene naphthalate) (PEN) have good optical transmittance in the visible range and solvent resistance, but their low T_g (80−150 °C) is unsuitable for high-temperature processing.[4−8]

Polyimides (PIs) are engineering plastics that have become important in the microelectronic industry as flexible circuitry carriers, stress buffers, interdielectric layers, and passivation layers. They have good thermal stability (high T_g of > 250 °C and low CTE of < 20 ppm/°C), a high decomposition temperature of > 400 °C, mechanical toughness, pliability, solvent resistance, and outstanding electrical properties. However, they are generally pale yellow to brown in color. For example, Kapton, the most well-known PI derived from pyromellitic acid dianhydride (PMDA) and 4,4′-diaminodiphenyl ether (ODA), has strong coloration from yellowish-brown to blackish-brown due to the characteristic absorption tailings in the visible region caused by the intra- and intermolecular charge transfer (CT) interactions of the polyimide backbones. In addition, ordered structures at the nanometer level also deteriorate the transparency in the UV/vis region due to Rayleigh scattering.

In this regard, many colorless and transparent PIs have been developed for applications as optical materials in the field of micro-optical components and waveguide circuits.[9−12] Although PIs prepared from alicyclic monomers of dianhydrides or diamines generally have good transparency in the visible region, their mechanical toughness is unsuitable for use as transparent and colorless substrates.[13−20] In contrast, fluorinated PIs, such as 6FDA/TFDB PI prepared from 2,2-bis(3,4-dicarboxyphenyl)-hexafluoropropane dianhydride (6FDA) and 2,2-bis(trifluoromethyl)-4,4′-diaminobiphenyl (TFDB), exhibit high transparency in the visible region, colorlessness, low dielectric constant, good solubility to polar organic solvents, and high thermal stability with T_g of > 300 °C.[21−29] These materials have been studied extensively as optical materials and colorless substrates. Despite these merits, these materials are difficult to synthesize and too expensive to be used as a substrate compared to other polymers. In addition, their CTE values of > 80 ppm/°C are too high for applications as substrates in electronic devices, while the CTE values of < 20 ppm/°C are generally required.

The refractive index and birefringence of PIs are also important properties for optical applications, such as flexible transparent substrates, microlens and optical waveguides. In particular, high refractive index polymers with low optical loss have been studied actively because polymers usually have a lower refractive index than inorganic materials. Therefore, high refractive polymer materials are essential for replacing inorganic materials in the field of optical devices, such as microlens and optical

*Corresponding authors. E-mail: csha@pusan.ac.kr (C.-S.H.); sando@polymer.titech.ac.jp (S.A.).

 Published on Web 06/24/2009

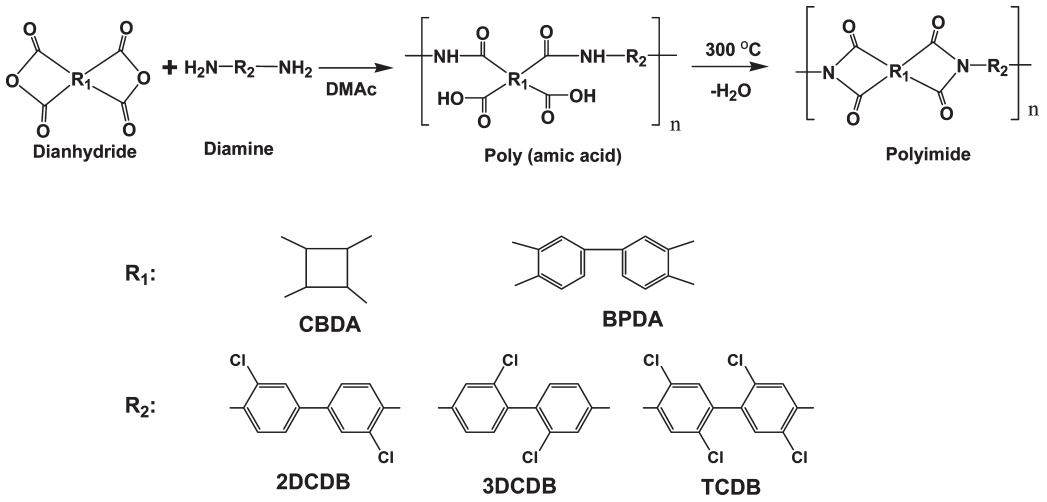

Figure 1. Preparation procedure of chlorinated PIs.

waveguide.[30−33] In this regard, many types of fluorine- or chlorine-containing PIs have been studied.[9,10] In particular, there are several reports on chlorinated PIs prepared using chlorinated dianhydrides or chlorinated diamines.[34−36] Zhubanov et al.[34] prepared new chlorinated PIs through single-step polycondensation of chlorinated tricyclodecenetetracarboxyl dianhydride with various diamines. Hariharan et al.[35] synthesized organo-soluble chlorinated polyimides based on chlorinated diamine, 4,4′-dichloro-3,3′-diaminobenzophenone. To the best of our knowledge, however, there are no reports of fully aromatic PIs containing no fluorine and exhibiting colorlessness over the entire visible region.

Therefore, in this study novel colorless chlorinated polyimides (PIs) were synthesized using three types of chlorinated benzidines with different molecular structures, such as 3,3′-dichlorobenzidine (2DCDB), 2,2′-dichlorobenzidine (3DCDB), and 2,2′,5,5′-tetrachlorobenzidine (TCDB), and rigid-structured dianhydrides such as 1,2,3,4-cyclobutanetetracarboxylic dianhydride (CBDA) and 3,3′,4,4′-biphenyltetracarboxylic dianhydride (BPDA). These materials exhibited good thermal and mechanical stability and a low CTE as well as good optical properties with high transparency and high refractive indices in the visible and near-infrared regions. Their optical properties, which depend significantly on the molecular structure of the PI main chains, and their thermal and mechanical properties were also characterized.

Experimental Section

Materials and Methods. 2,2′-Dichlorobiphenyl-4,4′-diamine (3DCDB) and 2,2′,5,5′-tetrachlorobiphenyl-4,4′-diamine (TCDB) were provided by Wakayama Seika Co. Ltd. 3,3′-Dichlorobiphenyl-4,4′-diamine (2DCDB) was provided by Fuji Film Co. Ltd. All the diamines were purified by recrystallization from ethyl acetate followed by sublimation under reduced pressure. 3,3′,4,4′-Biphenyltetracarboxylic dianhydride (BPDA) and *p*-phenylenediamine (PDA) were purchased from Wako Chemical and also purified by sublimation under reduced pressure. 1,2,3,4-Cyclobutanetetracarboxylic dianhydride (CBDA) provided by JSR Corp., and *N*,*N*-dimethylacetamide (DMAc, anhydrous) purchased from Aldrich were used as received. Six types of chlorinated PIs and a reference PI (BPDA/PDA PI) were prepared by thermal imidization of their corresponding precursors, poly(amic acid)s (PAAs). The PAAs were synthesized by addition polymerization of equimolar amounts of diamines and dianhydrides in DMAc. Each dianhydride was added to a diamine solution, dissolved with or without heating, and stirred at room temperature for 2−5 days. All procedures were carried out in a glovebox purged with nitrogen. DMAc solutions of the PAA precursors were spin-coated onto 3 in. diameter fused silica (amorphous SiO_2) substrates and imidized thermally under programmed curing conditions, where they were dried at 70 °C for 2 h, heated to 300 °C with several steps as shown in Figure 1, and kept at 300 °C for 1 h under a nitrogen flow. Finally, PI films with thicknesses of 10−20 μm were obtained. More details on the synthesis and characterization of PI films produced in this study are described in the Supporting Information.

Measurement. The attenuated total reflection−Fourier transform infrared (ATR-FTIR, Nicolet Avatar-320) spectra were obtained with 32 scans per spectrum at a 2 cm^{-1} resolution. A robust single-reflection accessory (Thunderdome, Spectra-Tech Co., Ltd.) with a germanium IRE (n = 4.0, incidence angle = 45°) was used for the ATR measurements. Thermogravimetric analysis (TGA) was performed on Shimadzu DTG-60 thermal analyzer. The samples were heated from 50 to 900 °C at a heating rate of 10 °C/min. Differential scanning calorimetry (DSC) was carried out with Shimadzu DSC-60 differential scanning calorimeter. The samples were heated from 50 to 400 at 10 °C min^{-1}. The coefficient of thermal expansion (CTE) was measured using a TA Instruments thermal mechanical analyzer (TMA) with a fixed load of 0.05 N and a heating rate of 10 °C min^{-1}. The TGA, DSC, and TMA measurements were conducted under a nitrogen flow. Mechanical (tensile) properties of the composite films were measured using a universal testing machine (UTM, Korea Apparel Testing & Research Institute) at a crosshead speed of 10 mm/min at room temperature. Each reported value is the average of five different measurements. The ultraviolet−visible (UV−vis) absorption spectra were obtained for the synthesized PI films with a thickness of 15 μm recorded with a single accumulation on a Hitachi U-3500 spectrophotometer optimized with a spectral width of 200−800 nm, a resolution of 0.5 nm, and a scanning rate of 120 nm min^{-1}. The excitation and fluorescent-emission spectra of the PI films were characterized using a Hitachi F-4500 fluorescence spectrophotometer with a resolution of 0.2 nm and a scanning rate of 240 nm min^{-1}. The film thickness, in-plane (n_{TE}), and out-of-plane (n_{TM}) refractive indices of the films formed on the silica substrates were measured using a prism coupler (Metricon, PC-2000) at wavelengths of 632.8, 845, and 1324 nm at room temperature. The mean refractive indices (n_{av}) were calculated as $n_{av}^2 = (2n_{TE}^2 + n_{TM}^2)/3$. The in-plane/out-of-plane birefringence (Δn) was calculated as $\Delta n = n_{TE} - n_{TM}$. The thicknesses of PI films were measured with a sensing-pin type surface profilometer (DEKTAK-III).

Results and Discussion

Molecular Structures. Figure 2 shows the three-dimensional molecular structures of the chlorinated PIs. The geometries

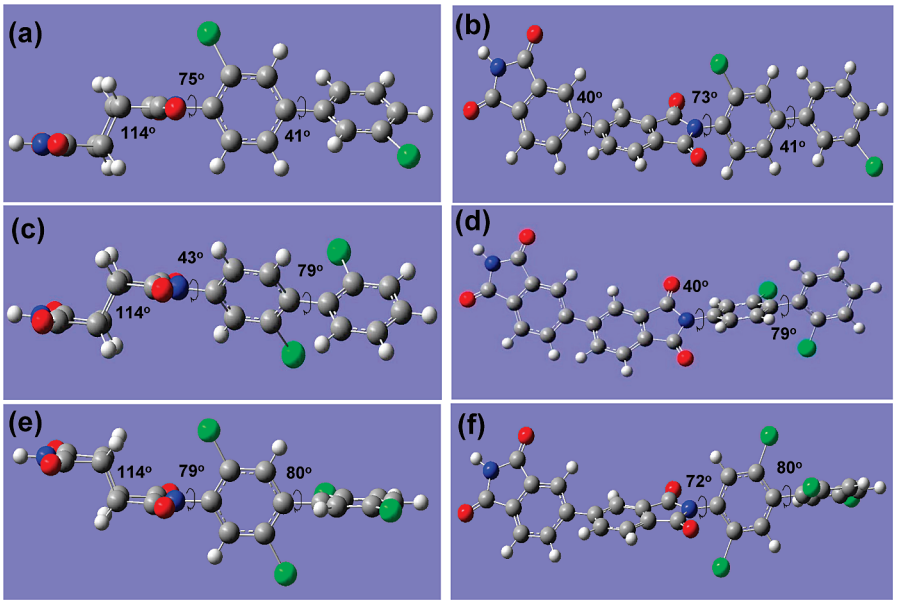

Figure 2. Molecular structures of the model compounds for chlorinated PIs. (a) CBDA/2DCDB; (b) BPDA/2DCDB; (c) CBDA/3DCDB; (d) BPDA/3DCDB; (e) CBDA/TCDB; (f) BPDA/TCDB. Gray, white, red, blue, and green of each molecular structure display C, H, O, N, and Cl, respectively. The geometries were optimized by the DFT (B3LYP/6-311G(d,p)) calculations, and the dihedral angles at the skeletal structures are shown in the figures.

were optimized by the density functional theory (DFT) calculations using a large basis-set function.[37−42] More details on the quantum chemical calculations are provided in the Supporting Information. CBDA synthesized by the photodimerization method was reported to have a cis−trans−cis stereostructure.[43] The distances between the plane of the methylene carbon atom estimated by the XRD patterns were 1.48, 1.51, 1.57, and 1.62 Å. Note that the steric hindrance caused by bulky chlorine atoms directly attached to the 2-, 3-, or 2,5-positions (numbered from the carbon close to amine) of the benzidine rings induces significant conformational distortion to the PI backbones. As shown in the figure, the dihedral angles between the benzene ring at the diamine moiety and the imide ring in 2DCDB-containing PIs (2DCDB/CBDA and 2DCDB/BPDA) and TCDB-containing PIs (TCDB/CBDA and TCDB/BPDA), which have bulky chlorines adjacent to the 5-membered imide rings, are 72°−79°, which are significantly higher than those 3DCDB-containing PIs (3DCDB/CBDA and 3DCDB/BPDA) without any chlorine atoms at the same position due to the steric hindrance caused by the bulky chlorines. Furthermore, the steric hindrance caused by the 3-, 5-positioned chlorines of 3DCDB and TCDB also distorted the molecular structure in the benzidine moieties significantly from ∼41° to ∼80°. The steric effect was more noticeable for the TCDB-containing PIs because they have two different types of steric hindrance: between the benzene ring and imide ring and between the two benzene rings in the diamine moiety. As a result, the four consecutive rigid rings (benzene and imide rings) along the main chains in the TCDB-containing PIs have significantly distorted conformations, in which the rings are almost perpendicular to each other.

Optical Transparency. Figure 3a shows the UV/vis absorption spectra of the PI films with a thickness of ∼15 μm. All PI films, except for BPDA/2DCDB and BPDA/3DCDB, were transparent and colorless in the visible region, while BPDA/2DCDB and BPDA/3DCDB were pale-yellowish in color. Table 1 summarizes the absorption edges (λ_E) estimated by the point where the absorption curve intersects a bisected line drawn through the intersection of the extrapolations of the two slopes. Note that the absorption edges of all PIs, except for BPDA/3DCDB, were observed below 400 nm, which are significantly shifted to a shorter wavelengths compared to those of the conventional aromatic PIs. For example, the absorption edge of BPDA/PDA PI, which is derived from BPDA dianhydride and *p*-phenylenediamine (PDA), was observed at ∼413 nm.

As shown in Figure 4, the optical transmission spectra of the PIs derived from alicyclic CBDA dianhydride show high transparency in the visible region. This is due to the weakened electron accepting properties of the imide moieties originating from the alicyclic nature of CBDA. The absence of benzene rings in the dianhydride and/or diamine moieties effectively suppresses the intra- or intermolecular CT interactions.[44] In addition, a fully aromatic PI derived from BPDA and TCDB produces a colorless PI film with an absorption edge of ∼377 nm. This is essentially due to the effect of steric hindrance caused by chlorine atoms, which significantly distorts the PI backbone, as shown in Figure 2. Therefore, the conformation of the main chain inhibits the conjugation of imide−phenyl and phenyl−phenyl bonds in the PI chains and weakens the intra- or intermolecular CT interactions. In contrast, significant CT interactions are widely observed in conventional aromatic PIs.[31] This is the reason why BPDA/2DCDB, BPDA/3DCDB, and BPDA/TCDB PIs exhibit shorter absorption edges than BPDA/PDA. Interestingly, the absorption edge of BPDA/2DCDB was observed at 397 nm, which is similar to that of BPDA/3DCDB (403 nm), demonstrating that the number of chlorine atoms has a greater influence on the optical properties than the position of the chlorine atoms in these chlorinated PIs.

It should be noted that the absorption edges observed for the TCDB-containing PIs were shifted to a shorter wavelength compared to those of the 2DCDB- and 3DCDB-containing PIs. This might be due to the decreased conjugation at the diamine moiety in the PI main chains. As shown in Figure 2, the optimized dihedral angle at the biphenyl moiety is increased from 41° for 2DCDB to 80° for TCDB, and that at the imide-ring structure is increased from 40° for 3DCDB to 70° for TCDB. Furthermore, the addition of electronegative chlorines to the skeletal structure of 2DCDB and 3DCDB significantly reduce the highest occupied molecular orbital (HOMO) levels of TCDB. These two factors may be the reasons why the calculated ionization

potentials of 2DCDB (6.94 eV) and 3DCDB (6.89 eV) are significantly lower than those of TCDB (7.09 eV), which suggests that the two chlorine substituted diamine have higher electron-donating properties than the four chlorine substituted diamine. This can induce bathochromic shifts (red shifts) in the absorption of PI films prepared from 2DCDB and 3DCDB. Second, the shorter absorption edges observed the TCDB-containing PIs might be due to the reduced intermolecular CT interactions caused by the four chlorine atoms in TCDB. The distorted conformations at the imide−phenyl and phenyl−phenyl bonds in the PIs derived from 2DCDB, 3DCDB, and TCDB should increase the intermolecular distances and free volumes. In addition, the bulky and spatially extended TCDB structures further increase and free volumes compared with 2DCDB, 3DCDB, and PDA. Accordingly, the intermolecular CT interactions are weakened, and the tailings of the absorption characteristic to conventional aromatic PIs might be reduced.

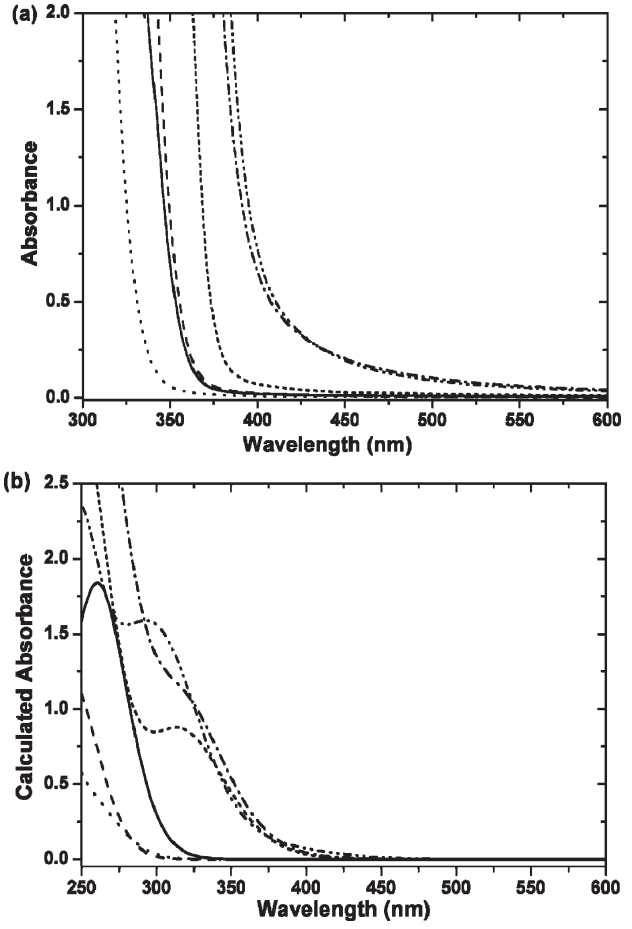

Figure 3. UV−vis absorption spectra (a) and calculated absorption spectra (b) of the chlorinated PIs. CBDA/2DCDB (—); CBDA/3DCDB (− − −); CBDA/TCDB (···); BPDA/2DCDB (−·−); BPDA/3DCDB (−··−); BPDA/TCDB (---).

Figure 3b displays the calculated absorption spectra of the PIs using the TD-DFT method. The significantly larger λ_E value observed for BPDA/2DCDB and BPDA/3DCDB than that of BPDA/TCDB was not reproduced in the calculations. Since the intermolecular CT interactions were not included in the calculations, the very close absorption edges in the calculated spectra of BPDA/2DCDB, BPDA/3DCDB, and BPDA/TCDB indicate that the tailing of the experimental absorptions to longer wavelengths for BPDA/2DCDB and BPDA/3DCDB are mainly caused by the intermolecular CT interactions. As stated above, the smaller torsion angle at the biphenyl moiety of 2DCDB and that at the imide-ring structure of 3DCDB could enhance the intermolecular CT as well as the intramolecular CT in the solid PI films.

Figure 4 shows the optical transmission spectra of the PI films in the visible region. The spectra are principally the same as those shown in Figure 3. However, it is important to understand the difference in the optical transparency at the longer wavelengths. As expected from its alicyclic nature, CBDA-containing PIs show good transparency with a transmittance >90% at 400 nm. Furthermore, it should be highly noted that BPDA/TCDB PI, a fully aromatic tetrachlorinated PI, also exhibited good transmittance of ~82% at 400 nm and with a > 90% average transmittance in the visible range. The high transparency of BPDA/TCDB PI is comparable to that of highly fluorinated 6FDA/TFDB PI. This is the highest transmittance in fully aromatic PIs reported. This shows that the judicious introduction of chlorine atoms to the diamine moiety of PIs, which has significant steric effects on the main chain, is quite effective in eliminating or at least reducing the characteristic coloration of aromatic PIs.

Thermal and Mechanical Properties. The thermal properties of the chlorinated PIs were evaluated by the glass transition temperatures (T_g), which was determined by differential scanning calorimetry (DSC) and by the decomposition temperatures with a 5% weight loss (T_d^5) observed by thermogravimetric analysis (TGA). The DSC thermograms

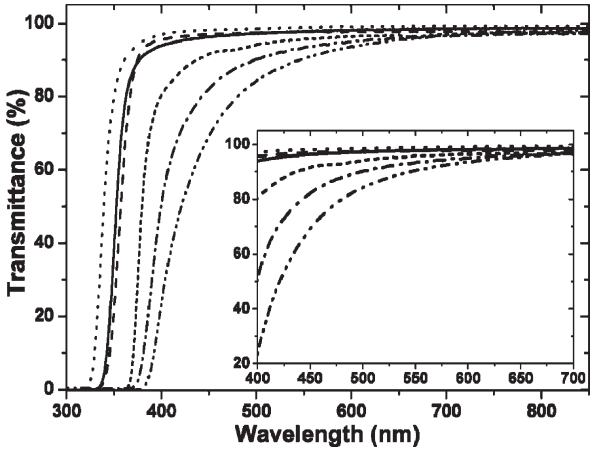

Figure 4. Optical transmission spectra of the chlorinated PI films. CBDA/2DCDB (—); CBDA/3DCDB (− − −); CBDA/TCDB (···); BPDA/2DCDB (−·−); BPDA/3DCDB (−··−); BPDA/TCDB (---). The inset shows the optical transmission spectra in the visible range.

Table 1. Molecular Orbital Energies (ε) of HOMO and LUMO, Energy Gaps ($\Delta\varepsilon$), Absorption Edges (λ_E), Excitation and Emission Peaks (λ_{ex}, λ_{em}) in the Fluorescence Spectra, Thermal Degradation Temperature of 5 wt % (T_d^5), Tensile Strength (σ), Modulus (E), and Elongation (ε_L)

polyimide	ε_{HOMO} [eV]	ε_{LUMO} [eV]	$\Delta\varepsilon$ [eV]	λ_E [nm]	λ_{ex} [nm]	Λ_{em} [nm]	T_d^5 [°C]	σ [MPa]	E [GPa]	ε_L [%]
CBDA/2DCDB	−7.07	−1.96	5.11	357	352	415	452			
CBDA/3DCDB	−7.06	−1.85	5.21	359	345	407	439			
CBDA/TCDB	−7.18	−1.89	5.29	333	333	381	439			
BPDA/2DCDB	−6.94	−3.13	3.81	397	361	457	539	104 ± 9	3.5 ± 0.5	4 ± 1
BPDA/3DCDB	−6.89	−3.20	3.81	403	351	459	560	129 ± 7	2.1 ± 0.2	8 ± 2
BPDA/TCDB	−7.09	−3.19	3.90	377	364	422	565	138 ± 7	2.3 ± 0.3	7 ± 2

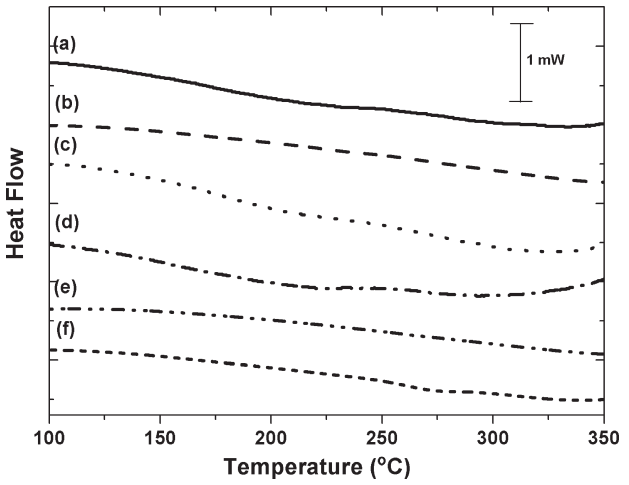

Figure 5. DSC thermograms of the chlorinated PIs: (a) CBDA/2DCDB; (b) CBDA/3DCDB; (c) CBDA/TCDB; (d) BPDA/2DCDB; (e) BPDA/3DCDB; (f) BPDA/TCDB.

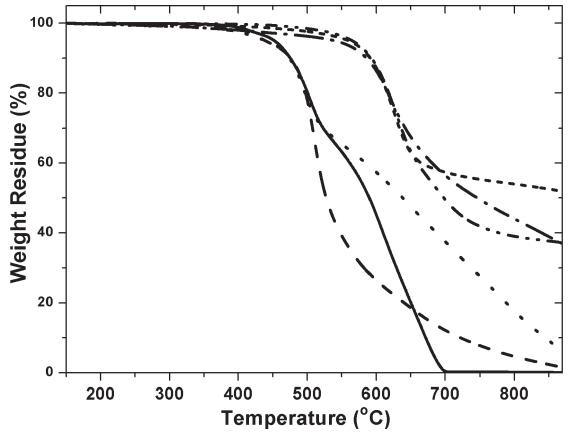

Figure 6. TGA curves of the chlorinated PIs: CBDA/2DCDB (—); CBDA/3DCDB (– – –); CBDA/TCDB (···); BPDA/2DCDB (–·–); BPDA/3DCDB (–··–); BPDA/TCDB (---).

of the PIs are presented in Figure 5. No significant changes were observed for all the PIs below 300 °C. In addition, no apparent glass transitions were detected up to their decomposition temperatures, which is due to their rigid molecular structures. Figure 6 shows the TGA curves of the chlorinated PIs. All PIs demonstrate good thermal stability without significant weight loss up to 400 °C. In particular, the fully aromatic PIs (BPDA/2DCDB, BPDA/3DCDB, and BPDA/TCDB) showed apparently better thermal stability with higher T_d[5] at ~540 °C than the alicyclic PIs whose T_d[5] appear at ~440 °C. The decomposition of the anhydride moieties of the PI chains generally appears at lower temperature than that of the diamine moieties, and the high chlorine content reduces the decomposition rate of PIs.

Furthermore, TMA analysis (Figure 7) demonstrates that the fully aromatic chlorinated PIs exhibit relatively low CTEs of 40−45 ppm °C^{-1} between 50 and 250 °C. The CTEs of these chlorinated PI films are almost half of that of 6FDA/TFDB PI (82 ppm °C^{-1}),[21] which was attributed to the rigid-rod structure of the main chain despite the bulky chlorine side groups. In addition, a low CTE is highly advantageous to apply as a material in optically transparent and thermally stable PI substrates for flexible displays, in which the polymer substrates need to be exposed to high temperature > 200 °C during the vacuum deposition processes of inorganic thin films.

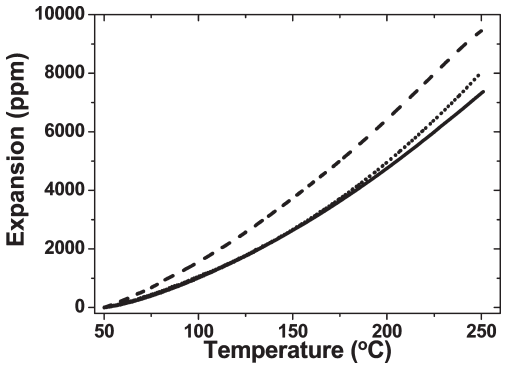

Figure 7. TMA curves of the aromatic chlorinated PI films: BPDA/2DCDB (—); BPDA/3DCDB (– – –); BPDA/TCDB (···).

All fully aromatic PIs derived from aromatic dianhydride (BPDA) and aromatic diamines (2DCDB, 3DCDB, and TCDB) have good pliability and toughness sufficient for applications in flexible substrates, while alicyclic diamine (CBDA) containing PIs are too brittle to make free-standing films. As shown in Table 1, the tensile strength and modulus of the PIs (BPDA/2DCDB, BPDA/3DCDB, and BPDA/TCDB) were observed at 104 ± 9, 129 ± 7, and 138 ± 7 MPa and at 3.5±0.5, 2.1±0.2, and 2.3±0.3 GPa, respectively. The chlorinated PIs exhibit enhanced mechanical properties compared to PMDA/ODA PI, which was fabricated under the same curing conditions and had a tensile strength and modulus of 101±5 MPa and 1.5±0.2 GPa, respectively. This is probably due to the rigid-rod-like structure of the PI main chains and bulky chlorine directly attached to the PI backbones.

Fluorescent Properties. Fluorescent spectroscopy is used widely to examine the electronic structures and aggregation states of polymers on account of its high sensitivity to microenvironmental changes in polymer matrices.[44] Figure 8 shows the one-dimensional excitation and emission spectra of the chlorinated PI films. All PI films showed an apparent fluorescent emission in the visible region. Table 1 lists the wavelengths of the excitation and emission peaks.

The PIs derived from alicyclic CBDA dianhydride showed fluorescent emission originating from their locally excited (LE) states, in which the electrons excited at the dianhydride moieties (S_1*) were relaxed to a similar location in the ground state. This can be characterized by the small Stokes shifts of 0.53, 0.55, and 0.47 eV for CBDA/2DCDB, CBDA/3DCDB, and CBDA/TCDB PIs, respectively. The Stokes shift was estimated from the difference in wavelength between the excitation and emission peaks. The excitation peak of CBDA/2DCDB PI appearing at 352 nm was red-shifted compared to that of CBDA/TCDB PI (333 nm), which coincides well with the red-shifted absorption edge at 357 nm of the former compared to the latter (333 nm). This also agrees with the smaller value of the calculated band gap for the CBDA/2DCDB (5.11 eV) than that for CBDA/TCDB (5.29 eV).

The PIs derived from aromatic BPDA (BPDA/2DCDB, BPDA/3DCDB, and BPDA/TCDB) show excitation peaks at 361, 351, and 364 nm and emission peaks at 457, 459, and 422 nm, and the calculated Stokes shifts were 0.73, 0.83, and 0.47 eV, respectively. The Stokes shifts of BPDA/2DCDB and BPDA/3DCDB are much larger than that of the BPDA/TCDB. The former value of 0.73−0.83 eV is typically observed in conventional aromatic PIs, in which significant charge transfer (CT) interactions induce efficient energy transfer from the LE state to the exited CT state. Figure 9

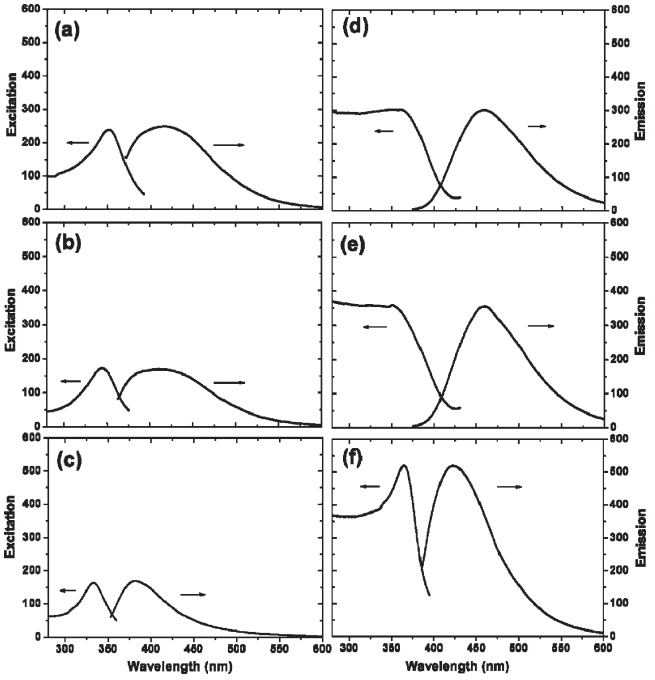

Figure 8. Excitation and fluorescent emission spectra of chlorinated PIs: (a) CBDA/2DCDB; (b) CBDA/3DCDB; (c) CBDA/TCDB; (d) BPDA/2DCDB; (e) BPDA/3DCDB; (f) BPDA/TCDB.

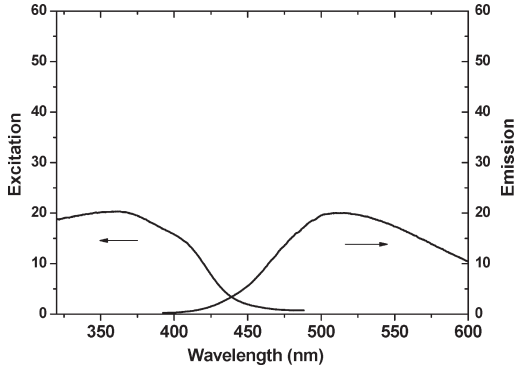

Figure 9. Excitation and fluorescent emission spectra of a conventional aromatic PI (BPDA/PDA).

shows the fluorescent emission spectra of a typical aromatic PI, BPDA/PDA, which exhibits a large Stokes shift of 0.92 eV with an excitation peak (368 nm) and emission peak (506 nm). The excited CT state is characterized by electron transfer from the electron-donating diamine moiety to the electron-accepting dianhydride moiety. In contrast, the electron excited from the ground state to the LE state stays at the dianhydride moiety because the LE state is close to the Franck−Condon state and the lowset unoccupied molecular orbital (LUMO) of PIs is generally located at the dianhydride moiety. The siginificant difference in electronic structures between the LE and CT states should be the main reason for the large Stokes shift observed in conventional aromatic PIs. In contrast, the Stokes shift of 0.47 eV observed for BPDA/TCDB is much closer to those of the CBDA-containing PIs with very weak CT interactions. In addition, BPDA/TCDB exhibits a sharper and stronger fluorescence peak than BPDA/2DCDB and BPDA/3DCDB. This suggests that fully aromatic BPDA/TCDB emits strong fluorescence, not from the CT state but from the LE state. In particular, this emission is considerably stronger than conventional aromatic PIs. These results can be explained by

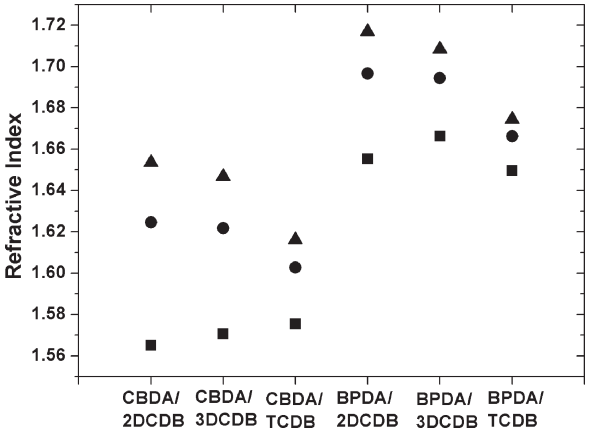

Figure 10. In-plane (n_{TE}, ▲), out-of-plane (n_{TM}, ■), and average refractive indices (n_{av}, ●) of the chlorinated PIs measured at a wavelength of 1324 nm. The average refractive index (n_{av}) was calculated as $n_{av}^2 = (2n_{TE}^2 + n_{TM}^2)/3$.

the steric effects caused by bulky chlorine atoms directly attached to the benzidine moiety of diamine. The distorted confirmations in the PI backbone not only reduce the imide−phenyl and phenyl−phenyl conjugations but also weaken the intra- or intermolecular CT interactions, which effectively decreases the Stokes shift and significantly enhances the fluorescence from the LE state. To the best of knowledge, this is the first example of the effective suppression of intra- and intermolecular CT interactions in fully aromatic PIs through the judicious introduction of chlorine atoms to the skeletal structures. In contrast, BPDA/2DCDB and BPDA/3DCDB PIs, which have a more planar biphenyl conformation, showed a broad and weak fluorescence peak with a larger Stokes shift than BPDA/TCDB PI. This fluorescence is demonstrated as a typical fluorescence from the excited CT state generated by the energy transfer from the LE states.

Refractive Indices and Birefringence. Figure 10 shows the refractive indices of the chlorinated PI films formed on Si substrates. The n_{TE} and n_{TM} represent the polarization-dependent refractive indices parallel and perpendicular to the film plane. As expected, the chlorine-containing aromatic PIs, such as BPDA/2DCDB, BPDA/3DCDB, and BPDA/TCDB, exhibit high n_{av} values > 1.70 at 632.8 nm due to the highly polarizable chlorine atoms. In particular, the n_{av} of 1.7317 observed for BPDA/2DCDB was significantly higher than that of conventional aromatic polyimides.[25] A very high n_{av} of 1.7616 was reported for a fully aromatic BPDA/PDA PI. However, this PI shows strong coloration and a large birefringence (0.1972). Furthermore, the n_{av} of 1.7018 observed for BPDA/TCDB is extraordinarily high for a colorless PI. The n_{av} of highly fluorinated colorless 6FDA/TFDB PI was 1.5418, which is 9.5% lower than that of BPDA/TCDB. Heavy halogens, such as chlorine, bromine, and iodine, increase the refractive index and dielectric constants of polymers. However, the refractive indices and birefringence of these PI films decreased with increasing chlorine content. These two phenomena can be explained by the more bulky structures of the TCDB-containing PIs significantly increasing their van der Waals volumes compared to the 2DCDB- or 3DCDB-containing PIs and also inhibiting dense molecular packing. Consequently, the TCDB-containing PIs inherently have a larger intermolecular volume, which is also consistent with the high optical transparency due to the significantly weakened intermolecular CT interactions, as discussed above. The calculated refractive indices for CBDA/2DCDB, CBDA/3DCDB,

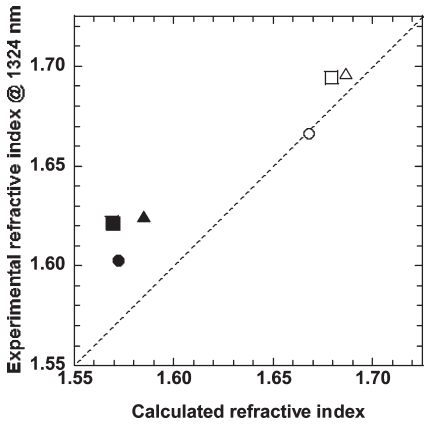

Figure 11. Comparison between the calculated and experimental average refractive indices (n_{av}) of the chlorinated PIs: CBDA/2DCDB (▲); CBDA/3DCDB (■); CBDA/TCDB (●); BPDA/2DCDB (Δ); BPDA/3DCDB (□); BPDA/TCDB (○).

Table 2. Calculated van der Waals Volumes (V_{vdw}), Molecular Polarizabilities (α), and Estimated Packing Coefficients (K_p) of the Chlorinated PIs[a]

calculated	V_{vdw} (Å^3)	α (Å^3)	α/V_{vdw}	K_P at $\lambda = \infty$
CBDA/2DCDB	317.67	42.54	0.1339	0.6238
CBDA/3DCDB	317.75	41.59	0.1309	0.6355
CBDA/TCDB	345.61	45.43	0.1314	0.6184
BPDA/2DCDB	403.63	61.38	0.1521	0.5976
BPDA/3DCDB	403.71	60.89	0.1508	0.6002
BPDA/TCDB	431.57	64.21	0.1488	0.5890

[a] The packing coefficients (K_p) were calculated as $(n_{av}^2-1)/(n_{av}^2+2) = (4\pi/3)K_p(\alpha_{av}/V_{vdw})$, where n_{av}, α_{av}, and V_{vdw} are the average refractive index, the average polarizability, and the van der Waals volume of the PIs, respectively.

CBDA/TCDB, BPDA/2DCDB, BPDA/3DCDB, and BPDA/TCDB at 632.8 nm were 1.6210, 1.5994, 1.6018, 1.7587, 1.7504, and 1.7299, respectively, in which a constant molecular packing coefficients (K_p) of 0.6 was assumed. As shown in Figure 11, the calculated n_{av} are approximately proportional to the experimental n_{av} values. It is reasonable that the PIs derived from CBDA show significantly lower refractive indices than those from BPDA, which is due to the aliphatic nature of CBDA. Although the calculations do not incorporate the effects of molecular packing, the 2DCDB-containing PIs show significantly higher refractive indices than the TCDB-containing PIs, indicating that the larger molecular volume of TCDB has a more dominant influence than the higher polarizability of the additional chlorines. Since it was reported that the molecular polarizabilities can be calculated using the DFT method,[45] the fact that the slope of the linear fitting (dashed line) in Figure 11 is slightly smaller than unity indicates that the PIs derived from BPDA have lower degrees of molecular packing than those from CBDA.

In addition, K_p values were estimated from the observed refractive indices and the calculated molecular polarizabilities (Table 2) to determine the average intermolecular distances and free volumes in TCDB-containing PIs.[45] This coefficient can be used as a measure of the molecular packing density of a PI. When the dianhydride structure is fixed, the K_p values estimated for the TCDB-containing PIs (e.g., 0.5890 for BPDA/TCDB) were significantly smaller than those of the 2DCDB- or 3DCDB-containing PIs (e.g., 0.6002 for BPDA/3DCDB), which agrees well with the tendency of refractive indices. This also supports that the increase in free volume caused by addition of chlorine is significant for TCDB.

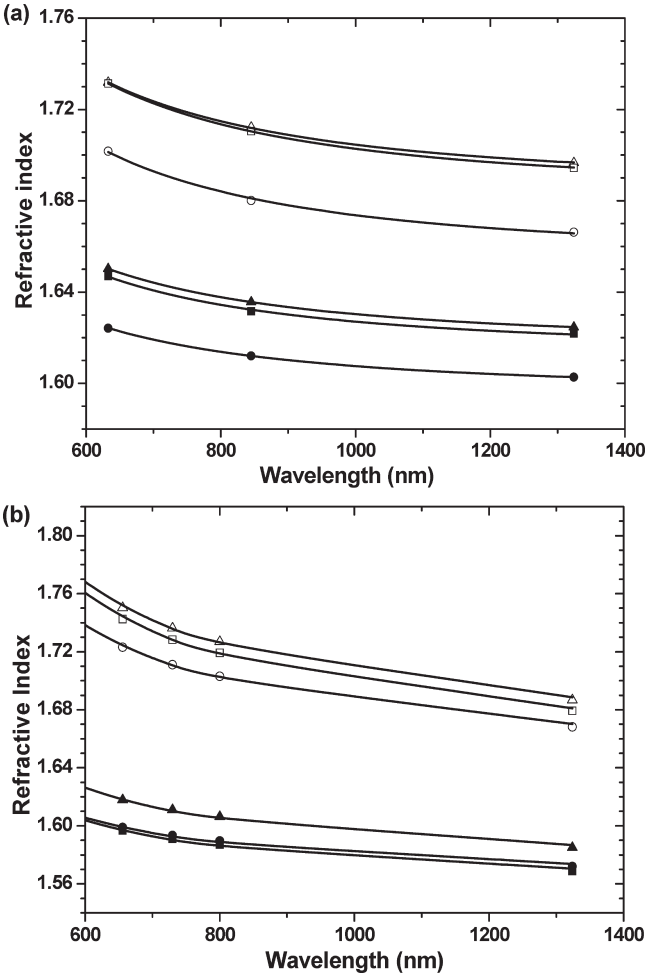

Figure 12. Wavelength dispersion of the (a) experimental and (b) calculated n_{av} values of the chlorinated PIs: CBDA/2DCDB (▲); CBDA/3DCDB (■); CBDA/TCDB (●); BPDA/2DCDB (Δ); BPDA/3DCDB (□); BPDA/TCDB (○). The experimental refractive indices were measured at three wavelengths of 632.8, 845, and 1324 nm, and the dispersion curves were fitted with the simplified Cauchy's formula, $n_\lambda = n_{inf} + (D/\lambda^2)$, where n_{inf} is the estimated refractive index at infinite wavelength and D is the coefficient of wavelength dispersion. The values of n_{inf} and D are listed in Table 3.

The anisotropy in the refractive index, which is generally called "birefringence", is also an important optical property for applications in waveguide devices, in which a high birefringence may degrade the transmission quality due to polarization-dependent losses.[11] The chlorinated PIs, particularly TCDB-containing PIs, exhibit significantly low in-plane/out-of-plane birefringence (Δn) despite their rigid molecular structures and high refractive indices. Conventional PIs with rigid structures generally show large birefringence. For example, the Δn values of BPDA/PDA, PMDA/TFDB, and PMDA/ODA PIs at 632.8 nm are 0.1972, 0.1368, and 0.0841, respectively. In contrast, the small Δn values of 0.0449 and 0.0279 for CBDA/TCDB and BPDA/TCDB PIs are significant and noteworthy. This also reflects the highly hindered molecular conformations between PI chains in the TCDB-containing PIs. Owing to the high transparency, high refractive indices, and low birefringence, BPDA/TCDB PI can be a promising candidate not only for the optical waveguide materials but also for thin film (< 0.2 μm thick) lens materials for CCD/C-MOS lens arrays.

Figure 12a,b shows the wavelength dispersion of the experimental and calculated n_{av} values of the chlorinated

Table 3. Refractive Indices (n_{TE}, n_{TM}) and Birefringence (n) of the Chlorinated PIs Measured at 1324 nm, Coefficients of Wavelength Dispersion (D), Refractive Indices at Infinite Wavelength (n_∞), and Abbe Numbers in the Visible and Near-Infrared Region (V_{VIS} and V_{NIR}, Respectively)[a]

polyimide	n_{TE}	n_{TE}	n_{av}	Δn	D	n_∞	V_{VIS}	V_{NIR}
CBDA/2DCDB	1.6536	1.5651	1.6246	0.0885	13 246	1.6171	25.9	24.9
CBDA/3DCDB	1.6468	1.5707	1.6218	0.0761	13 129	1.6139	26.0	25.0
CBDA/TCDB	1.6162	1.5755	1.6027	0.0407	11 160	1.5964	29.5	28.5
BPDA/2DCDB	1.7169	1.6553	1.6966	0.0616	18 226	1.6864	21.2	20.3
BPDA/3DCDB	1.7084	1.6663	1.6945	0.0421	19 146	1.6836	20.2	19.3
BPDA/TCDB	1.6745	1.6497	1.6663	0.0248	18 490	1.6552	20.1	19.1

[a] The average refractive indices (n_{av}) were calculated as $n_{av}^2=(2n_{TE}^2 + n_{TM}^2)/3$. The in-plane/out-of-plane birefringence (Δn) was calculated as $\Delta n = n_{TE} - n_{TM}$. The V_{VIS} and V_{NIR} were calculated as $V_{VIS} = (1-n_{589})/(n_{486} - n_{656})$ and $V_{NIR} = (1 - n_{845})/(n_{633} - n_{1324})$, where the n_λ represents the refractive index measured at a wavelength of λ.

PIs. The Abbe number (V), which is commonly used to estimate the wavelength dependence of the refractive indices of optical materials, was calculated in the visible (V_{VIS}) and NIR region (V_{NIR}) using the fitted curve in Figure 12, and the results are listed in Table 3. The smaller V values, which correspond to a higher degree of wavelength dispersion, observed for the PIs derived from BPDA compared to those from CBDA can be explained by the high refractive indices and lower optical transparency in the UV/vis region of the former PIs, as evidenced by the larger V values. The most transparent CBDA/TCDB exhibits the largest V values as expected. However, the colorless BPDA/TCDB PI shows a slightly smaller V_{NIR} value (19.1) than the pale-yellowish BPDA/2DCDB (20.3) and BPDA/3DCDB (19.3), which is caused by the larger increase in n_{av} at 632.8 nm. Further purification of the monomers and optimization of the imidization procedures should be effective in improving the large dispersion with high V values. As shown in Figure 12b, the trends of the wavelength dispersion of the experimental n_{av} values are reproduced well by the wavelength-dependent calculated n_{av} values. The significant increase in n_λ at shorter wavelengths corresponds to the normal refractive index dispersion near the absorption edges. Although there were systematic errors between the experimental and calculated n_{av} values, the DFT calculations predict that the n_{av} values of PIs derived from BPDA can be >1.74 at the visible shorter wavelengths (ca. 400−550 nm). It is also noteworthy that such high refractive indices can be obtained from aromatic PIs without introducing sulfur atoms or heavy halogens like bromine or iodine.

Conclusions

Novel chlorinated polyimides (PIs) with rigid structures were synthesized. All PI films except for BPDA/2DCDB and BPDA/3DCDB PIs showed good optical transparency in the visible region. In particular, BPDA/TCDB PI, a fully aromatic PI, was colorless and transparent with a transmittance of ~82% at 400 nm and with an average transmittance of >90% in the visible region. This is the highest transparency ever reported for unfluorinated fully aromatic PIs and is comparable to that of highly fluorinated 6FDA/TFDB PI.

All the PIs exhibited high thermal stability without apparent changes in the DSC curves below the decomposition temperatures. BPDA-containing aromatic PIs showed significantly high thermal stability with 5% degradation temperatures of >540 °C and relatively low CTEs of 40−45 ppm °C^{-1} between 50 and 250 °C. In particular, the BPDA/TCDB PI film, a colorless PI film, exhibited a low CTE of ~44 ppm °C^{-1} between 50 and 250 °C, which is almost half that of colorless fluorinated 6FDA/TFDB PI, as well as good pliability and toughness suitable for applications to flexible substrates.

All PI films, except for BPDA/2DCDB and BPDA/3DCDB, showed fluorescent emissions from the LE state, while BPDA/2DCDB and BPDA/3DCDB showed emission from the charge transferred exited CT state generated by energy transfer from the LE state. In particular, the emission observed for a fully aromatic BPDA/TCDB is much stronger than those of other fully aromatic PIs. This is due to the suppression of intra- and intermolecular CT interactions as a result of significant steric hindrance caused by chlorines. As indicated by the DFT calculations, the imide−phenyl bonds in all PIs should be distorted significantly by the chlorines at the 2-, 3-, and 5-positions of the benzidine moiety and the biphenyl linkages.

The high refractive indices of >1.70 at 623.8 nm were obtained for the PIs derived from BPDA and chlorinated diamines. In particular, the n_{av} of 1.7317 observed for BPDA/2DCDB at 632.8 nm was considerably higher than that observed for conventional aromatic polyimides, and the n_{av} of 1.7018 observed for BPDA/TCDB is extraordinarily high as a colorless PI. The n_{av} of colorless 6FDA/TFDB PI is 1.5418, which is 9.5% lower than that of BPDA/TCDB.

In conclusion, colorless, flexible, and thermally stable PI films suitable for applications as flexible films in advanced electronic and optical devices can be produced by controlling the steric hindrance in the main chain of PIs through the judicious introduction of chlorine atoms.

Acknowledgment. The authors thank for the Core-University Program between Japan (Tokyo Tech) and Korea (KAIST) which is financially supported through Japan Society for the Promotion of Science (JSPS) and Korea Science and Engineering Foundation (KOSEF). The work was partly supported by the KOSEF Grant funded by the Ministry of Education, Science and Technology, Korea (MEST) (Acceleration Research Program (No. 2009-0078791), a grant from the Fundamental R&D Program for Core Technology of Materials funded by the Ministry of Knowledge Economy, Korea, and the Brain Korea 21 Project.

Supporting Information Available: Details of synthesis of chlorinated PIs, FT-IR characterization of the chlorinated PIs with ATR-FTIR spectra of the chlorinated PIs, and quantum chemical calculation. This material is available free of charge via the Internet at http://pubs.acs.org.

References and Notes

(1) Nathan, A.; Chalamala, B. R. *Proc. IEEE* **2005**, *93* (7−8).
(2) Allen, K. J. *Proc. IEEE* **2005**, *93*, 1394.
(3) Choi, M. C.; Kim, Y.; Ha, C. S. *Prog. Polym. Sci.* **2008**, *33*, 581.
(4) MacDonald, B. A.; Rollins, K.; Eveson, R.; Rakos, K.; Rustin, B. A.; Handa, M. *Mater. Res. Soc. Symp. Proc.* **2003**, *769*, H9.3.1.
(5) Gelinck, G. H.; Huitema, H. E. A.; Mil, M. V.; Veenendaal, E. V.; Lieshout, P. J. G. V.; Touwslager, F. J. *SID Dig.* **2005**, *36*, 6.
(6) Yan, M.; Kim, T. W.; Erlat, A. G.; Pellow, M.; Foust, D. F.; Liu, J.; Schaepkens, M.; Heller, C. M.; Connelee, P. A. M.; Feist, T. P.; Dugga, A. R. *Proc. IEEE* **2005**, *93*, 1468.
(7) Lim, H.; Bae, C. M.; Kim, Y. K.; Park, C. H.; Cho, W. J.; Ha, C. S. *Synth. Met.* **2003**, *135−136*, 49.
(8) Lewis, J. S.; Weaver, M. S. *IEEE J. Sel. Top. Quantum Electron.* **2004**, *10*, 45.
(9) Ando, S. *J. Photopolym. Sci. Technol.* **2004**, *17*, 219.
(10) Han, K.; Lee, H.-J.; Rhee, T. H. *J. Appl. Polym. Sci.* **1999**, *74*, 107.
(11) Han, K.; Kim, D. B.; Jang, W. H.; Rhee, T. H. *Jpn. J. Appl. Phys.* **1999**, *38*, L1249.
(12) Liu, J.; Nakamura, Y.; Ogura, T.; Shibasaki, Y.; Ando, S.; Ueda, M. *Chem. Mater.* **2008**, *20*, 273.
(13) Mathews, A. S.; Kim, I.; Ha, C. S. *J. Polym. Sci., Polym. Chem.* **2006**, *44*, 5354.
(14) Mathews, A. S.; Kim, I.; Ha, C. S. *Macromol. Res.* **2007**, *15*, 114.
(15) Jin, H. S.; Chang, J. H.; Kim, J. C. *Macromol. Res.* **2008**, *16*, 503.

(16) Yamada, M.; Kusama, M.; Matsumoto, T.; Kurosaki, T. *Macromolecules* **1993**, *26*, 4961.
(17) Itamura, S.; Yamada, M.; Tamura, S.; Matsumoto, T.; Kurosaki, T. *Macromolecules* **1993**, *26*, 3490.
(18) Matsumoto, T.; Kurosaki, T. *Macromolecules* **1997**, *30*, 993.
(19) Kato, J.; Seo, A.; Shiraishi, S. *Macromolucules* **1999**, *32*, 6400.
(20) Matsumoto, T. *Macromolecules* **1999**, *32*, 4933.
(21) Matsuura, T.; Hasuda, Y.; Nishi, S.; Yamada, N. *Macromolecules* **1991**, *24*, 5001.
(22) Lim, H. T.; Cho, W. J.; Ha, C. S.; Ando, S.; Kim, Y. K.; Park, C. H.; Lee, K. H. *Adv. Mater.* **2002**, *14*, 1275.
(23) Park, H. J.; Park, J. W.; Jeong, S. Y.; Ha, C. S. *Proc. IEEE* **2005**, *93*, 1447.
(24) Terui, Y.; Ando, S. *Appl. Phys. Lett.* **2003**, *83*, 4755.
(25) Ando, S.; Watanabe, Y.; Matsuura, T. *Jpn. J. Appl. Phys.* **2002**, *41*, 5254.
(26) Sato, Y.; Yoshida, M.; Ando, S. *J. Photopolym. Sci. Technol.* **2006**, *19*, 297.
(27) Matsuura, T.; Yamada, N.; Nishi, S.; Hasuda, Y. *Macromolecules* **1993**, *26*, 419.
(28) Feiring, A. E.; Auman, B. C.; Wonchoba, E. R. *Macromolecules* **1993**, *26*, 2779.
(29) Hougham, G. H.; Tesoro, G.; Shaw, J. *Macromolecules* **1994**, *27*, 3642.
(30) You, N. H.; Suzuki, Y.; Yorifuji, D.; Ando, S.; Ueda, M. *Macromolecules* **2008**, *41*, 6361.
(31) Su, H. W.; Chen, W. C. *J. Mater. Chem.* **2008**, *18*, 1139.
(32) Liu, J.; Nakamura, Y.; Suzuki, Y.; Shibasaki, Y.; Ando, S.; Ueda, M. *Macromolecules* **2007**, *40*, 7902.
(33) Liu, J.; Nakamura, Y.; Shibasaki, Y.; Ando, S.; Ueda, M. *Macromolecules* **2007**, *40*, 4614.
(34) Zhubanov, B. A.; Kravtsovtsova, V. D.; Mukhamedova, R. F. *Russ. J. Appl. Chem.* **2004**, *77*, 1835.
(35) Hariharan, R.; Bhuvana, S.; Sarojadevi, M. *High Perform. Polym.* **2006**, *18*, 163.
(36) Han, K.; You, K.; Jang, W. H.; Rhee, T. H. *Macromol. Chem. Phys.* **2000**, *201*, 747.
(37) Ando, S.; Fujigawa, T.; Ueda, M. *Jpn. J. Appl. Phys.* **2002**, *41*, L105.
(38) Gaussian 03, Revision D.02. Gaussian, Inc., Wallingford, CT, 2004.
(39) Slonimskii, G.; Askadskii, A.; Kitaigodorodskii, A. *Polym. Sci. USSR* **1970**, *A12*, 556.
(40) Bondi, A. *J. Phys. Chem.* **1964**, *68*, 441.
(41) Ando, S. *J. Photopolym. Sci. Technol.* **2006**, *19*, 351.
(42) Terui, Y.; Ando, S. *J. Photopolym. Sci. Technol.* **2005**, *18*, 337.
(43) Suzuki, H.; Abe, T.; Takaishi, K.; Narita, M.; Hamada, F. *J. Polym. Sci., Part A: Polym. Chem.* **2000**, *38*, 108.
(44) Hasegawa, M.; Horie, K. *Prog. Polym. Sci.* **2001**, *26*, 259.
(45) Terui, Y.; Ando, S. *J. Polym. Sci., Part B: Polym. Phys.* **2004**, *42*, 2354.